Cancer Chemother Pharmacol (2002) 50: 419–428
DOI 10.1007/s00280-002-0511-x

ORIGINAL ARTICLE

**John Carl Panetta · Yuri Yanishevski · Ching-Hon Pui
John T. Sandlund · Jeffrey Rubnitz · Gaston K. Rivera
Raul Ribeiro · William E. Evans · Mary V. Relling**

A mathematical model of in vivo methotrexate accumulation in acute lymphoblastic leukemia

Received: 21 March 2002 / Accepted: 17 July 2002 / Published online: 24 September 2002

Abstract Methotrexate (MTX) is one of the most widely used drugs for the treatment of childhood acute lymphoblastic leukemia (ALL). Interindividual differences in lymphoblast accumulation of MTX and its active metabolites, methotrexate polyglutamates (MTXPG), may contribute to the effectiveness of treatment among ALL subtypes. To better understand these differences in MTXPG accumulation, we developed a model to characterize the cellular influx and efflux of MTX, formation of MTXPG by the addition of glutamyl residues catalyzed by FPGS (folylpolyglutamate synthetase), and cleavage of glutamyl residues from MTXPG by GGH (γ-glutamyl hydrolase). The model was fitted to in vivo intracellular MTXPG concentrations measured serially in leukemic blasts from 20 newly diagnosed patients with ALL treated with 24-h intravenous infusions of MTX. The observed median concentrations of total MTXPG at 44 h was higher in B-lineage than in T-cell ALL (1706 vs 518 pmol/10^9 cells, $P < 0.025$), consistent with the higher estimated Vmax for FPGS activity in B-lineage vs T-lineage blasts (414 vs 93 pmol/10^9 cells/h, $P < 0.008$). Simulations based on the model-estimated parameters indicated greater accumulation of MTX, MTXPGs ($MTXPG_{2-7}$) and total MTX ($MTXPG_{1-7}$) with longer MTX infusions and with higher MTX doses, with the highest concentrations in hyperdiploid B-lineage, intermediate in non-hyperdiploid B-lineage, and lowest in T-cell ALL. These differences provide mechanistic and treatment insights for lineage and ploidy differences in MTXPG accumulation in human leukemia cells in vivo.

Keywords Pharmacokinetics · Pharmacodynamics · Folylpolyglutamate synthetase · γ-Glutamyl hydrolase · Reduced folate carrier

This work was supported by Cancer Center CORE grants CA21765 and CA78224, by a Center of Excellence grant from the State of Tennessee, and by American Lebanese Syrian Associated Charities (ALSAC).

J.C. Panetta · Y. Yanishevski · C.-H. Pui · J.T. Sandlund
J. Rubnitz · G.K. Rivera · R. Ribeiro · W.E. Evans
M.V. Relling (✉)
St. Jude Children's Research Hospital,
332 North Lauderdale St., Memphis, TN 38105-2794, USA
E-mail: mary.relling@stjude.org
Tel.: +1-901-4952348
Fax: +1-901-5256869

C.-H. Pui · J.T. Sandlund · J. Rubnitz · G.K. Rivera
R. Ribeiro · W.E. Evans · M.V. Relling
University of Tennessee, Memphis, TN 38101, USA

Introduction

Methotrexate (MTX) is used extensively in the treatment of children with acute lymphocytic leukemia (ALL) [5, 7, 8, 11, 26, 31, 34, 35, 40]. MTX and its intracellular polyglutamate metabolites (MTXPG) inhibit the enzymes dihydrofolate reductase (DHFR), thymidylate synthase, glycinamide ribonucleotide transformylase and aminoimidazole carboxamide ribonucleotide transformylase, all of which are needed for either thymidylate synthesis or de novo purine synthesis [1, 2, 9, 27, 42, 44]. Multiple therapy-related and patient-related prognostic factors affect the outcome of childhood ALL. Although the cure rate for childhood ALL now exceeds 80% in some trials, MTX resistance may contribute to treatment failure in some patients [6, 18, 28]. MTX and MTXPG accumulation in ALL blasts is highly variable among patients [41], differs by ALL lineage and ploidy [41, 45, 46], is influenced by MTX dosage [41], and is related to the antileukemic effects of MTX [27, 45, 46]. To determine possible causes for low accumulation of MTXPGs, we developed a mathematical model to describe intracellular concentrations of MTX and its metabolites in ALL blasts studied in vivo in children with ALL.

Several biological processes govern MTX and MTXPG concentrations intracellularly. At extracellular MTX concentrations less than 20 μM, the main pathway for cell entry is via active transport through the reduced folate carrier (RFC) [44]. At very low concentrations (< 0.1 μM), MTX transport may be facilitated by the folate receptor [21, 22]. Passive diffusion is thought to be

most relevant at higher extracellular concentrations of MTX ($>20\ \mu M$), and may account for about half the influx at extracellular MTX concentrations of 200 μM [44]. MTX is anabolized by folylpolyglutamate synthetase (FPGS), which sequentially adds glutamyl groups to MTX, forming polyglutamate chains up to six or seven glutamates long. The polyglutamates are removed (hydrolyzed) by γ-glutamyl hydrolase (GGH) [16, 33, 36, 39, 48]. MTXPG are stronger inhibitors of DHFR, thymidylate synthase, glycinamide ribonucleotide transformylase, and aminoimidazole carboxamide ribonucleotide transformylase than MTX [1], and these larger molecules cannot easily efflux from the cell [13, 29]. Thus, there are numerous mechanisms by which higher concentrations of MTXPG may be associated with greater antileukemic effects [2, 6, 18, 27, 41, 45].

We have previously compared in vivo $MTXPG_{1-7}$ concentrations in bone marrow blasts obtained at a fixed time-point (44 h from the start of MTX exposure) after two doses of MTX (1 g/m^2 over 24 h i.v. vs 30 mg/m^2 orally every 6 h for six doses) [41]. These studies established that total MTXPG accumulation is higher with the higher dose, but there is substantial interpatient variability in MTXPG accumulation. Hyperdiploid B-lineage ALL have the highest MTXPG accumulation, putatively related to increased expression of RFC [4], and T-lineage have the lowest MTXPG accumulation, partly due to lower FPGS activity [3]. However, these studies examined MTXPG accumulation at a single time-point, and did not include serial data on MTXPG concentrations over time. In the present study, we measured and modeled the time-course of MTXPG in serially collected samples in vivo, in children with ALL treated with a range of intravenous MTX dosages. The model provides insights into the mechanisms of lineage and ploidy differences in MTXPG accumulation in ALL blasts in vivo, and may be useful for predicting effects of various dosage regimens of MTXPG.

Methods

Patients and drug administration

Between August 1998 and July 1999 48 children with newly diagnosed ALL were enrolled on study protocol Total XIV and received up-front MTX. Of these patients, 20 had adequate circulating blasts for serial studies of MTXPG concentrations.

At diagnosis, patients were randomized to receive 24-h MTX i.v. infusion with dosages adjusted to target steady-state plasma concentration (C_{pss}) of 2.5, 5, 10, 17.5, 30, 45, 70, or 90 μM MTX. These concentrations encompass average MTX doses of 250 mg/m^2 to 8 g/m^2, doses that have been used in ALL trials [34]. To achieve these targeted concentrations, blood samples were drawn at the end of a 20-min loading dose and at 3 h after the start of the MTX infusion and the plasma MTX concentrations were measured by the Abbottbase TDx-FPIA II assay (Abbott Diagnostics, Irving, Tx.). Based on estimates of clearance using these two measurements (as determined using a first-order two-compartment model and the maximum *a posteriori* probability (MAP) parameter estimation method implemented in the ADAPT II software [10]), a dose adjustment was made at 5 h to achieve the desired MTX C_{pss}. The dose range to achieve the targeted C_{pss} for each of the 20 patients was between 209 and 7676 mg/m^2. All treatments were followed at 48 h by leucovorin rescue.

Measurement of MTX and MTXPG

Blood was obtained from each patient at 20 min, 3 h, 23 h, and 44 h after the start of MTX infusion, plasma MTX assayed as described above, and final pharmacokinetic parameters were estimated via MAP using all four time-points. These final parameters were used in the modeling described below.

Leukemic blast cells were isolated by Ficoll-Hypaque gradient and washed three times with a solution of Hepes, Hanks' buffered salt solution, and heparin. The final cell yield was determined by hemocytometer and the percent viability by trypan blue exclusion. MTX and six polyglutamated metabolites were separated by HPLC and quantitated by radioenzymatic assay, as we have previously described [41]. Separate calibration curves were used for quantitation of MTX and each polyglutamate metabolite. The limit of detection of this assay was 0.02 pmol/10^6 cells. All results are expressed as picomoles MTXPG per 10^9 cells. MTXPGs were also measured in bone marrow blasts obtained 44 h from the start of MTX.

Development of model

A mathematical model based on the models of White and Mikulecky [44] and Morrison and Allegra [30] was developed to characterize the kinetics of intracellular MTX and MTXPG. Model assumptions were as follows. (1) Accumulation of MTXPG was grouped as either $MTXPG_2$-$MTXPG_7$ or $MTXPG_2$-$MTXPG_3$ (short chain) and $MTXPG_4$- $MTXPG_7$ (long chain). The subscript denotes the number of glutamates attached to each MTX molecule. (2) Active transport (via the RFC) was assumed to be the primary influx pathway and was modeled with a Michaelis-Menten term. (3) Passive influx was considered minor at plasma MTX concentrations $<20\ \mu M$ [44]. Also, active and passive influx were mathematically indistinguishable given only plasma and intracellular MTX concentrations. Therefore, first-order passive influx was fixed to the rate 0.4 l/h, as previously reported [44]. (4) Efflux was modeled as a first-order process and only $MTXPG_1$ (MTX) was permitted to efflux from the cell [13, 29]. (5) DHFR concentration was not estimated, as it was assumed to be less than MTXPG concentration during the 44 h of the experiment [23, 30, 44] and the data did not allow us to distinguish DHFR from uptake or efflux. (6) FPGS activity was modeled as a Michaelis-Menten reaction. (7) GGH activity was modeled as a first-order process [30]. (8) Intracellular MTX was assumed to have no influence on extracellular MTX, because the amount of intracellular MTX was much less than extracellular MTX at the relatively early time-points studied. Furthermore, extracellular MTX was modeled independently with a two-compartment pharmacokinetic model. These pharmacokinetic parameters were then fixed for each patient based on their individual data, and incorporated to provide the source of MTX to the intracellular MTXPG model.

With these assumptions, we tested the following two models. The first described the time-course of the intracellular concentrations of the parent drug (MTX) and the sum of all the polyglutamates ($MTXPG_{2-7}$) (Fig. 1a).

$$\frac{dMTXPG_1}{dt} = \frac{V_{m-1}MTX}{K_{m-1} + MTX} + K_pMTX - k_{eff}MTXPG_1 - \frac{V_{m-FPGS}MTXPG_1}{K_{m-FPGS} + MTXPG_1} + K_{GGH}MTXPG_{2-7}$$

$$\frac{dMTXPG_{2-7}}{dt} = \frac{V_{m-FPGS}MTXPG_1}{K_{m-FPGS} + MTXPG_1} - K_{GGH}MTXPG_{2-7}$$

The second model describes the intracellular concentrations of the parent drug (MTX), short-chain polyglutamates ($MTXPG_{2-3}$), and long-chain polyglutamates ($MTXPG_{4-7}$) (Fig. 1b).

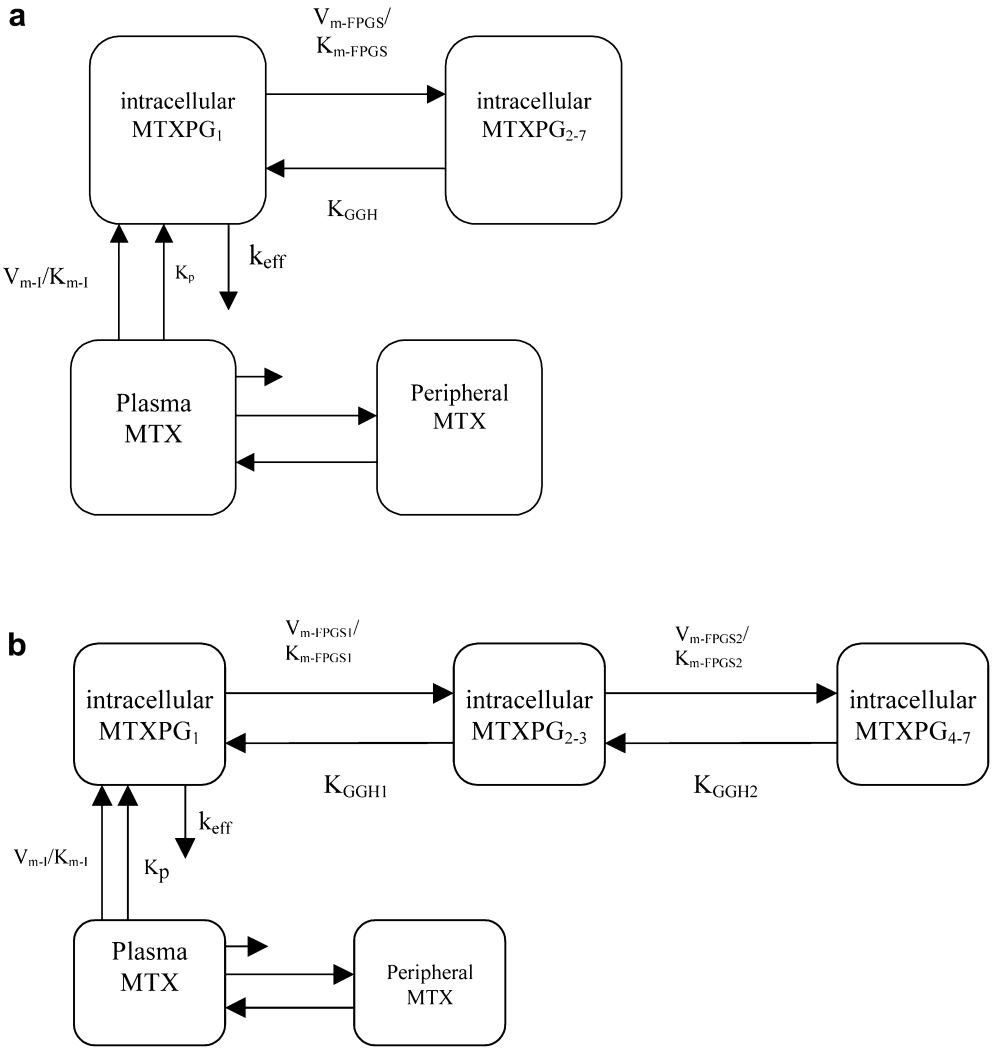

Fig. 1. **a** Two-compartment model for blast MTXPG accumulation. The parameters are defined as follows. $V_{m\text{-}I}$ and $K_{m\text{-}I}$ the Michaelis-Menten parameters for active (RFC) influx, K_p the first-order passive influx parameter, k_{eff} the first-order efflux parameter, $V_{m\text{-}FPGS}$ and $K_{m\text{-}FPGS}$ the Michaelis-Menten parameters for FPGS activity, K_{GGH} the first-order GGH activity parameter. Standard two-compartment plasma MTX model depicted at bottom. **b** Three-compartment model for blast MTXPG accumulation. The parameters are defined as follows. $V_{m\text{-}I}$ and $K_{m\text{-}I}$ the Michaelis-Menten parameters for active (RFC) influx, K_p the first-order passive influx parameter, k_{eff} the first-order efflux parameter, $V_{m\text{-}FPGSi}$ and $K_{m\text{-}FPGSi}$ the Michaelis-Menten parameters for FPGS activity, K_{GGHi} the first-order GGH activity parameter. The subscript $i = 1,2$ represents the parameters for the $MTXPG_{2-3}$ and $MTXPG_{4-7}$ compartments, respectively. Standard two-compartment plasma MTX model depicted at bottom

$$\frac{dMTXPG_1}{dt} = \frac{V_{m-I}MTX}{K_{m-I} + MTX} + K_pMTX - k_{eff}MTXPG_1 - \frac{V_{m-FPGS1}MTXPG_1}{K_{FPGS1} + MTXPG_1} + K_{GGH1}MTXPG_{2-3}$$

$$\frac{dMTXPG_{2-3}}{dt} = \frac{V_{m-FPGS1}MTXPG_1}{K_{m-FPGS1} + MTXPG_1} - K_{GGH1}MTXPG_{2-3} + \frac{V_{m-FPGS2}MTXPG_{2-3}}{K_{FPGS2} + MTXPG_{2-3}} + K_{GGH2}MTXPG_{4-7}$$

$$\frac{dMTXPG_{4-7}}{dt} = \frac{V_{m-FPGS2}MTXPG_{2-3}}{K_{m-FPGS2} + MTXPG_{2-3}} - K_{GGH2}MTXPG_{4-7}$$

The variables were defined as follows. MTX the extracellular concentration of methotrexate, $MTXPG_1$ the intracellular concentration of methotrexate, $MTXPG_{2-7}$ the sum of the concentrations of $MTXPG_2$–$MTXPG_7$, $MTXPG_{2-3}$ the concentration of short-chain MTXPG ($MTXPG_2 + MTXPG_3$), and $MTXPG_{4-7}$ the sum of the concentrations of long-chain MTXPG ($MTXPG_4$–$MTXPG_7$). The parameters were defined as follows: V_{m-I} and K_{m-I} the Michaelis-Menten parameters for active (RFC) influx, K_p the first-order passive influx parameter, k_{eff} the first-order efflux parameter, $V_{m-FPGSi}$ and $K_{m-FPGSi}$ the Michaelis-Menten parameters for FPGS activity, and K_{GGHi} the first-order GGH activity parameter. All parameters are constant with the exception of V_{m-I} and V_{m-FPGS} which are increasing functions of MTX dose [3].

Several secondary model parameters were also estimated, including those related to intracellular $MTXPG_1$ retention:

- Intrinsic influx to efflux ratio ($Ratio_{IE}$): $V_{m-I}/K_{m-I}/k_{eff}$ (pmol/μM). This is the measure of the net influx-to-efflux activity, accounting for the activity of the RFC (V_{m-I}/K_{m-I}) and the efflux process (k_{eff}).
- Maximum active transport intracellular $MTXPG_1$ accumulation (MAX_{pg1}): V_{m-I}/k_{eff} (pmol/10^9 cells). This is the maximum possible accumulation of $MTXPG_1$ assuming an infinitely large dose. This assumed no passive diffusion; otherwise, the maximum accumulation could be infinite.

and those related to intracellular $MTXPG_{2-7}$ retention:

- Intrinsic FPGS to GGH ratio ($Ratio_{FG}$): $V_{m\text{-}FPGS}/K_{m\text{-}FPGS}/K_{GGH}$ (unitless). This is the measure of the net FPGS-to-GGH activity accounting for the affinity for the enzyme ($K_{m\text{-}FPGS}$).
- Maximum $MTXPG_{2-7}$ accumulation (MAX_{pg2-7}): $V_{m\text{-}FPGS}/K_{GGH}$ (pmol/10^9 cells). This is the maximum possible accumulation of $MTXPG_{2-7}$ given an infinitely large dose (i.e. this is an upper bound on accumulation of $MTXPG_{2-7}$).

Data analysis

Model parameters were estimated from serial ALL blast samples obtained from 20 patients with newly diagnosed ALL, all of whom had data from all four peripheral blood blast samples. Parameters

for the two models were initially estimated by maximum likelihood estimation via ADAPT II [10]. Due to the limited amount of data, some of the data sets were not fitted well by this method, as determined by large sums of squares, Akaike information criteria (AIC), or poor visual fit. All data sets were then reanalyzed using the MAP Bayesian estimation technique as implemented in ADAPT II. To constrain parameter estimates, a prior estimate was determined using the mean and covariance matrix based on the initial maximum likelihood-derived parameter estimates. Acceptable fits (as determined by a reduction in the sum of squares, generalized information criterion (GEN-IC), or an acceptable visual fit) were obtained with all the data sets analyzed. ALL lineage, ploidy, and dose-dependent differences in the parameter estimates were compared by the Kruskal-Wallis ANOVA, the Mann-Whitney *U*-test, or generalized linear modeling.

Results

Patients

Of the 48 patients randomized to target steady-state MTX plasma concentrations of 2.5, 5, 10, 17.5, 30, 45, 70, or 90 μM, 20 had an adequate number of circulating leukemic blasts for serial studies of MTXPG concentrations (Table 1). Bone marrow blast concentrations of MTXPG were measured in 37 (7 B-lineage hyperdiploid, 22 B-lineage nonhyperdiploid, and 8 T-lineage) of 48 patients, including all 20 with serial blast samples.

Figure 2 shows the plasma MTX concentration vs time for a typical patient (B-lineage hyperdiploid, MTX dose 839 mg/m^2) along with the pharmacokinetic model fit of the data.

Comparison of two- and three-compartment models

Because the three-compartment model is more complex and contains more parameters, it is mathematically more difficult to accurately estimate its parameters. Therefore, we first performed a model discrimination analysis to determine whether the three-compartment model (which separated long-chain from short-chain MTXPGs) performed better at fitting the data than did the two-compartment model (which pooled $MTXPG_{2-7}$ in a single compartment). Figure 2b, c shows a fit to a representative patient using both the two- and the three-compartment models. The median sum of squares was 27% higher in the two-compartment model compared to the three-compartment model. However, in 37% of the patients, the sum of squares for the three-compartment model was higher than that of the two-compartment model. In addition, the median GEN-IC was 37% higher for the three-compartment compared to the two-compartment model, indicating greater parsimony for the simpler model. Given that there was a high correlation between $MTXPG_{2-3}$ and $MTXPG_{4-7}$ in all three subtypes (B-lineage hyperdiploid $r = 0.97$, $P < 0.05$; B-lineage nonhyperdiploid $r = 0.83$, $P < 0.05$; T-lineage $r = 0.98$, $P < 0.05$; all subtypes $r = 0.89$, $P < 0.05$; Fig. 3), the superior performance of the two-compartment model was not surprising. Therefore, we used the two-compartment model for the remainder of the analysis.

Differences among ALL subtypes

We compared the estimated model parameters among the three different ALL subtypes (Table 2). Median influx for all ALL subtypes were similar, whereas the affinity for influx was greatest among the hyperdiploid B-lineage blasts, and the median influx to efflux ratio ($Ratio_{IE}$) was approximately tenfold higher in B-lineage hyperdiploid ALL compared to the other two subtypes ($P < 0.05$). The median $V_{M\text{-}FPGS}$ was 4.4-fold higher in B-lineage blasts than in T-lineage blasts ($P < 0.01$) and the median K_{GGH} was 1.9-fold higher in nonhyperdiploid vs hyperdiploid ALL ($P < 0.05$). Hence, the maximum accumulation of polyglutamates (MAX_{pg2-7}) was fourfold higher in B-lineage than in T-lineage blasts ($P < 0.01$; Fig. 4).

The parameters describing influx ($V_{m\text{-}I}$), and FPGS activity ($V_{m\text{-}FPGS}$) were dose-dependent (Fig. 5). Although it is possible that the relationship between FPGS activity and dose is saturable, over the range of doses available in this study, a linear relationship was observed. Influx and FPGS activity both increased with dose ($P < 0.05$ and $P < 0.035$, respectively). As previously found experimentally in vivo [3], the increase in FPGS activity was greater with B-lineage compared to T-lineage ($P < 0.00075$). In particular, at a dose of 1 g/m^2, FPGS activity increased 150% and 21% in B- and T-lineage, respectively, over the predicted untreated activity. These results are consistent with higher polyglutamate accumulation in patients with B-lineage ALL [41].

Table 1. Patient demographics

	Subtype (lineage, ploidy)		
	B-lineage hyperdiploid	B-lineage nonhyperdiploid	T-lineage
n	5	10	5
Sex (male/female)	2/3	2/8	2/3
Race (African American/Caucasian)	0/5	2/8	3/2
MTX dose (mg/m^2)			
Median	1190	2418	1132
Range	209–3960	229–7676	368–5335
MTX C_{pss} achieved (μM)			
Median	14.0	40.1	18.8
Range	3.13–83.4	6.27–109.4	6.33–86.9

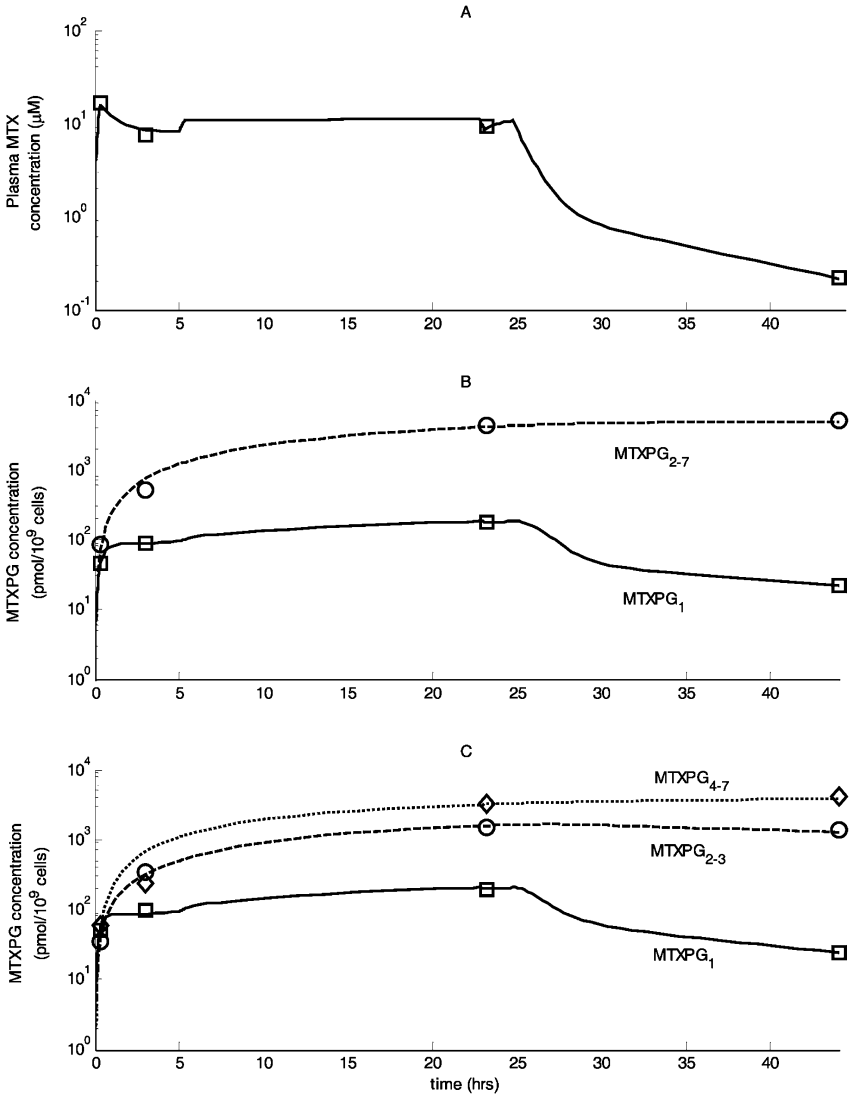

Fig. 2. **a** Plasma MTX concentration vs time for a typical patient (B-lineage hyperdiploid, MTX dose 839 mg/m^2). *Open squares* measured concentrations, *solid line* model simulation using a first-order two-compartment pharmacokinetic model. **b** Peripheral blast intracellular MTXPG concentration vs time for a typical patient. *Open squares* measured $MTXPG_1$ concentration, *open circles* measured $MTXPG_{2–7}$ concentration, *solid line* two-compartment model simulation of $MTXPG_1$, *dashed line* two-compartment model simulation of $MTXPG_{2–7}$. **c** Peripheral blast intracellular MTXPG concentration vs time for a typical patient. *Open squares* measured $MTXPG_1$ concentration, *open circles* measured $MTXPG_{2–3}$ concentration, *open diamonds* measured $MTXPG_{4–7}$ concentration, *solid line* three-compartment model simulation of $MTXPG_1$, *dashed line* three-compartment model simulation of $MTXPG_{2–3}$, *dotted line* three-compartment model simulation of $MTXPG_{4–7}$

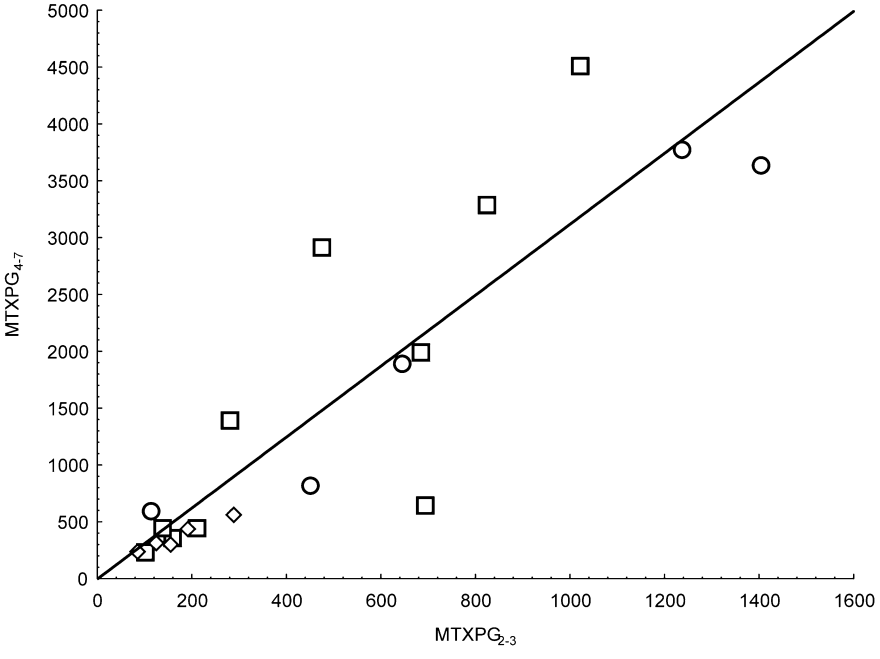

Fig. 3. Relationship between short-chain ($MTXPG_{2–3}$, pmol/10^9 cells) and long chain ($MTXPG_{4–7}$, pmol/10^9 cells) polyglutamates categorized by ALL subtype. *Solid line* regression line ($r = 0.88$, $P < 0.05$), *open circles* B-lineage hyperdiploid, *open squares* B-lineage nonhyperdiploid, *open diamonds* T-lineage

Table 2. Median (range) primary and secondary parameter estimates. Combined B-lineage pools data from B-lineage hyperdiploid and B-lineage nonhyperdiploid. *P*-values comparing B hyperdiploid-, B nonhyperdiploid- and T-lineages were derived from Kruskal-Wallis ANOVA; *P*-values comparing B-lineage to T-lineage and B-lineage nonhyperdiploid to B-lineage hyperdiploid were derived from the Mann-Whitney *U*-test

	B-lineage			T-lineage ($n=5$)	*P*-value		
	Hyperdiploid (BH) ($n=5$)	Nonhyperdiploid (BN) ($n=10$)	Combined (B) ($n=15$)		BH-BN-T	B-T	BN-BH
Primary parameters							
$V_{m\text{-}I}$ (pmol/10^9 cells/h)	674.9 (1418)	1273 (5223)	933.3 (5223)	595.8 (1386)	>0.1	>0.1	>0.1
$K_{m\text{-}I}$ (μM)	0.4 (13.4)	3.5 (29.3)	3.1 (30.1)	0.74 (8.8)	>0.1	>0.1	>0.1
k_{eff} (l/h)	3.4 (21.7)	6.4 (23.1)	5.3 (23.5)	6.1 (17.6)	>0.1	>0.1	>0.1
$V_{m\text{-}FPGS}$ (pmol/10^9 cells/h)	302.0 (340.8)	670.4(1502)	414.5 (1549)	93.48 (145.1)	<0.01	<0.01	>0.1
$K_{m\text{-}FPGS}$ (pmol/10^9 cells)	0.01 (7.8)	1.6 (83.7)	1.6 (84.1)	7.8 (48.1)	>0.1	>0.1	$0.05<P<0.1$
K_{GGH} (l/h)	0.10 (0.2)	0.28 (2.9)	0.18 (3.0)	0.18 (0.13)	$0.05<P<0.1$	>0.1	<0.05
Secondary parameters							
$Ratio_{IE}$	501.0 (669.0)	39.7 (124.6)	44.5 (692.1)	61.9 (575.1)	$0.05<P<0.1$	>0.1	<0.05
MAX_{pg1} (pmol/10^9 cells)	199.7 (546.0)	161.3 (1277)	162.5 (1310)	84.1 (221.3)	>0.1	>0.1	>0.1
MAX_{pg1} (μM)[a]	0.80	0.65	0.65	0.34			
$Ratio_{FG}$	72662 (197724)	860.6 (7083)	1053 (198565)	62.0 (41784)	<0.05	$0.05<P<0.1$	<0.01
$MAX_{pg2\text{–}7}$ (pmol/10^9 cells)	1986 (14091)	2236 (5720)	1986 (14274)	486.0 (848.3)	<0.05	<0.01	>0.1
$MAX_{pg2\text{–}7}$ (μM)[a]	7.9	8.9	7.9	1.9			
Actual accumulation							
$MTXPG_{2\text{–}7}$ (pmol/10^9 cells)							
23 h	1805 (8175)	847.1 (6331)	1423 (8647)	414.9 (750.0)	<0.05	<0.05	>0.1
44 h	2544 (4407)	1511 (5194)	1676 (5194)	459.0 (527.6)	<0.05	<0.05	>0.1
$MTXPG_{1\text{–}7}$ (pmol/10^9 cells)							
23 h	2146 (8656)	873.3 (5912)	1579 (9085)	505.2 (877.2)	<0.05	<0.05	>0.1
44 h	2603 (4397)	1535 (5220)	1706 (5220)	517.9 (539.9)	<0.05	<0.05	>0.1

[a]Conversion to micromoles per liter based on 250 fl/cell

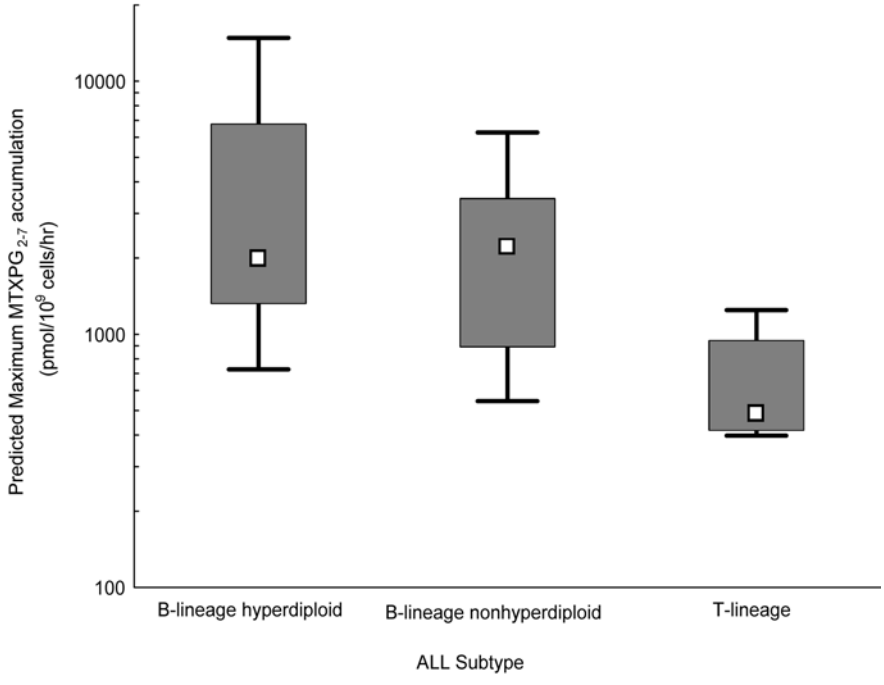

Fig. 4. Model-predicted maximum $MTXPG_{2\text{–}7}$ accumulation (pmol/10^9 cells per h) grouped by subtype, not including parent $MTXPG_1$. The *boxes* represent the 25–75% quartiles, the *square* in the boxes represents the median, and the *whiskers* represent the range. The median MTX doses (mg/m^2) were 1190, 2418, 1132 for B-lineage hyperdiploid, B-lineage nonhyperdiploid, and T-lineage, respectively

Predictions

To illustrate the predictions of the model and the parameter estimates, we plotted the observed data for MTX dose vs the measured 44-h peripheral blast concentrations of intracellular $MTXPG_1$ and $MTXPG_{2\text{–}7}$ and compared them to the model-predicted estimates for the three ALL subtypes. Although there was extensive variability in the data, the model accurately described observed data (Fig. 6). To give greater context for the model predictions, the model simulations were also compared to intracellular $MTXPG_1$ and $MTXPG_{2\text{–}7}$

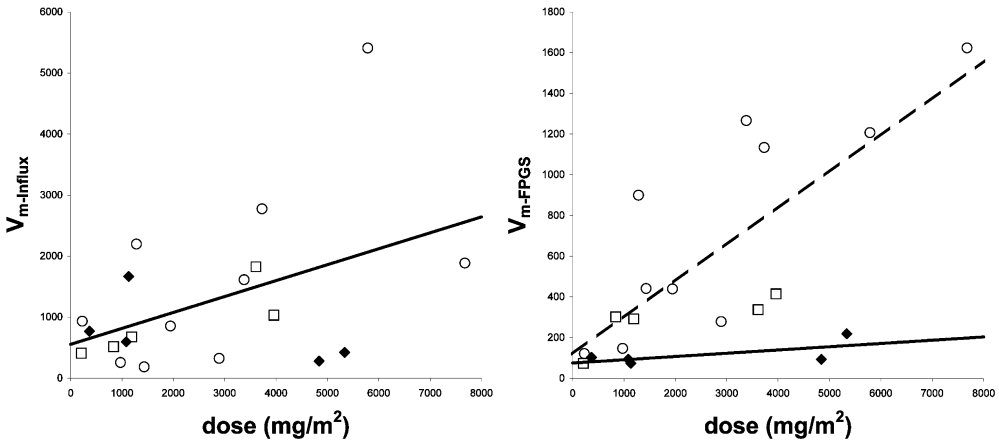

Fig. 5a, b. Regression of dose vs estimated model parameters. **a** MTX dose (mg/m^2) vs $V_{m\text{-}I}$ (maximum influx rate, pmol/10^9 cells per h; $r^2 = 0.2$, $P < 0.05$. **b** MTX dose (mg/m^2) vs $V_{M\text{-}FPGS}$ (maximum FPGS rate, pmol/10^9 cells per h). *Dashed line* regression line for B-lineage results ($r^2 = 0.6$, $P < 0.0005$), *solid line* regression line for T-lineage results ($r^2 = 0.4$, $P > 0.1$), *open circles* B-lineage hyperdiploid, *open squares* B-lineage nonhyperdiploid, *solid diamonds* T-lineage

concentrations measured in ALL blasts in bone marrow aspirates from 37 patients enrolled on the Total XIV protocol and concentrations of MTXPG1 and $MTXPG_{2\text{–}7}$ in bone marrow blasts from 144 patients enrolled on the Total XIIIA protocol of SJCRH (26 B-lineage hyperdiploid, 101 B-lineage nonhyperdiploid, and 17 T-lineage) who received MTX. Each of these patients was treated with MTX and had MTXPGs measured by the same method as those used for the peripheral blasts from patients on the Total XIV protocol. The model also predicted these bone marrow MTXPG concentrations reasonably well, as indicated in Fig. 6.

Differences due to drug infusion time

Based on the median estimated parameters in Table 2, the model predicted that infusion time would have a substantial effect on the 44-h accumulation $MTXPG_1$ and a lineage-dependent effect on the 44-h accumulation of $MTXPG_{2\text{–}7}$. The least effect of MTX infusion length on total MTXPG accumulation was observed in blasts from patients with B-lineage hyperdiploid ALL and the greatest effect was observed in patients with T-lineage ALL. In particular, T-lineage ALL were predicted to have a 28% increase in $MTXPG_{1\text{–}7}$ accumulation when the infusion time was increased from 4 h to 24 h, whereas only a 3–7% increase in $MTXPG_{1\text{–}7}$ accumulation was predicted in B-lineage ALL (Table 3).

Differences due to MTX dose

The model was also used to estimate the effects of dose (with a fixed 24-h infusion) on 44-h MTXPG accumulation (Fig. 7). Increasing dose past 2500 mg/m^2 caused little increase in MTXPG accumulation. In particular, increasing dose from 2500 to 5000 mg/m^2 caused a 6% (B-lineage hyperdiploid), 10% (B-lineage nonhyperdiploid), and 13% (T-lineage) increase in $MTXPG_{1\text{–}7}$ accumulation. In addition, we observed that T-lineage $MTXPG_{1\text{–}7}$ accumulation was always less than B-lineage $MTXPG_{1\text{–}7}$ accumulation at doses up to 10 g/m^2, indicating that an increase in MTX dose (assuming the same infusion time) would not be sufficient to increase MTXPG accumulation in T-lineage ALL to levels obtained in B-lineage ALL (Fig, 7), but the higher the MTX dose, the greater the MTXPG concentrations in T-lineage ALL.

Discussion

MTXPG accumulation was ALL subtype-dependent, with the greatest accumulation seen in B-lineage hyperdiploid ALL, followed by B-lineage nonhyperdiploid ALL, and lowest among T-lineage ALL (median accumulation of $MTXPG_{2\text{–}7}$ at 44 h: 2544, 1511, 459 pmol/10^9 cells respectively, $P < 0.05$), consistent with our previous observations with lower doses of MTX [27, 41]. This result is of importance to childhood ALL because MTXPG accumulation has been correlated with event-free survival and short-term antileukemic effects [27, 45]. In fact, several mathematical models have shown that a considerable accumulation of MTX is needed to compete with dihydrofolate [20, 42, 44]. To better understand the mechanisms for the observed lineage- and ploidy-related differences in MTX and MTXPG accumulation, we have modeled the time course of in vivo MTX accumulation and related it to biochemical factors known to influence MTX intracellular disposition. Our data allow for the first in vivo model of MTX disposition in leukemic blasts.

The influx, efflux, and GGH activity parameters determined in vivo in patients with ALL are comparable to previously reported estimates in in vitro and ex vivo studies [12, 20, 25, 30, 33, 37, 38, 43]. This lends additional support to the structural pharmacokinetic model we used for our in vivo data in patients. Our estimates for FPGS ($V_{m\text{-}FPGS}$ and $K_{m\text{-}FPGS}$) were lower than previously reported estimates in in vitro and ex vivo studies [3, 24, 25, 37, 38]. In an effort to address this difference, we modeled the data while constraining $K_{m\text{-}FPGS}$ to be near the literature-reported levels (mean 52 μM with a CV of 54%). However, this constraint

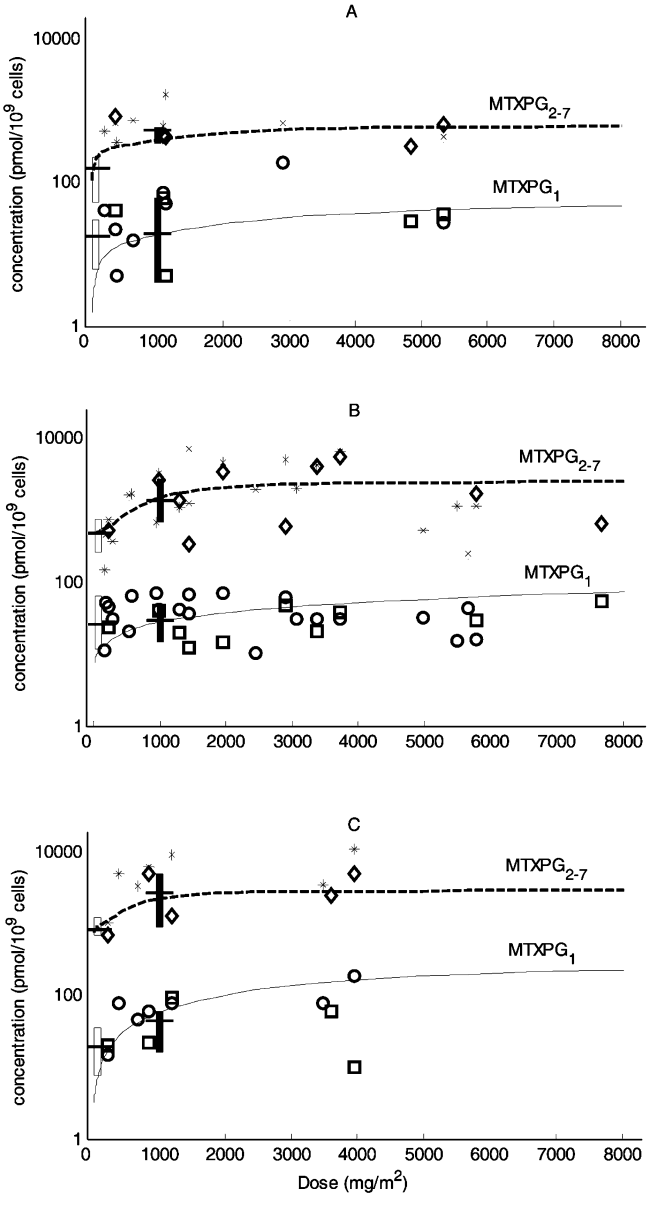

Fig. 6a–c. MTX dose vs in vivo 44-h intracellular $MTXPG_1$ and $MTXPG_{2-7}$ concentration *Solid line* $MTXPG_1$ model, *dashed line* $MTXPG_{2-7}$ model, *open squares* $MTXPG_1$ peripheral blast concentration, *open circles* $MTXPG_1$ bone marrow blast concentration, *open diamonds* $MTXPG_{2-7}$ peripheral blast concentration, *asterisks* $MTXPG_{2-7}$ bone marrow blast concentration. *Vertical bars* represent 25–75% quartiles and *horizontal bars* represent medians of MTXPG in bone marrow blasts treated with either low-dose (*open bars* 180 mg/m^2) or high-dose (*closed bars* 1000 mg/m^2) MTX in a previous study from our laboratory [27, 41]. **a** T-lineage; **b** B-lineage nonhyperdiploid; **c** B-lineage hyperdiploid

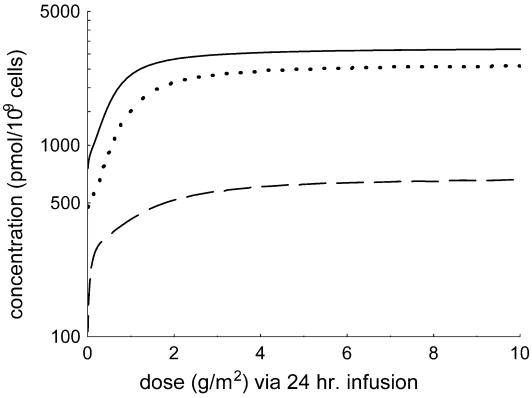

Fig. 7. Simulation of MTX dose (via a 24-h infusion) vs model-estimated 44-h $MTXPG_{1-7}$ concentration using the median model parameters listed in Table 2. *Solid line* B-lineage hyperdiploid, *dotted line* B-lineage nonhyperdiploid, *dashed line* T-lineage

resulted in a substantially worse fit – the sum of squares was typically an order of magnitude higher than when FPGS parameters were not constrained. One explanation for the differences is that in in vitro and ex vivo studies FPGS parameters were determined using higher substrate MTX concentrations (up to 250 μM) whereas the intracellular concentrations of MTX in the current study were lower (up to approximately 40 μM). Because it appears that $V_{M\text{-}FPGS}$ increases in a dose-dependent fashion after MTX [3] (Fig. 5), it is possible that the lower $V_{M\text{-}FPGS}$ and $K_{M\text{-}FPGS}$ that we observed were due to the fact that measurements were made at lower, more pharmacologic concentrations of MTX.

Morrison and Allegra [30] developed a mathematical model of MTX polyglutamation for intact MCF-7 breast cancer cells. Our model is similar, except that we considered FPGS activity to follow Michaelis-Menten kinetics, whereas they considered it to be linear. Our in vivo parameters for influx, efflux, and GGH were comparable to those measured in intact MCF-7 cells [30].

Differing parameter estimates among ALL subtypes may account for lineage- and ploidy-related differences in MTXPG accumulation. Low influx was more common among blasts from patients with relapsed compared to newly diagnosed ALL [19]. Greater MTXPG accumulation was observed in B-lineage blasts that had higher RFC expression, which was greater in hyperdiploid than in nonhyperdiploid blasts [4]. It has been suggested that differences in influx are in the affinity ($K_{m\text{-}I}$) rather than the maximum activity of the RFC

Table 3. Percentage increase in MTXPG concentrations at 24 and 44 h predicted with short (4-h) vs long (24-h) infusion lengths of the same total dosage (1 g/m^2). The percentages were determined as the percent increase achieved by a 24-h over a 4-h infusion

Time after start of MTX infusion (h)	B-lineage				T-lineage	
	Hyperdiploid		Nonhyperdiploid			
	24	44	24	44	24	44
$MTXPG_1$	72	117	470	126	121	118
$MTXPG_{1-7}$	3	2	19	6	15	25
$MTXPG_{2-7}$	0.4	3	2	7	7	28

($V_{m\text{-}I}$) [20]. Our data would tend to support that notion, because $K_{m\text{-}I}$ tended to be lowest for B-lineage hyperdiploid blasts (Table 2). We also found that the ratio of influx to efflux, (i.e. Ratio_{IE}), was about 12.5 times higher in B-lineage hyperdiploid blasts than B-lineage nonhyperdiploid blasts and about 8 times higher than T-lineage blasts, consistent with greater MTXPG accumulation in hyperdiploid and B-lineage than in T-cell blasts [41, 45, 46].

Our estimates of $V_{m\text{-}FPGS}$ differed significantly between B-lineage and T-cell ALL, with the greatest capacity in B-lineage nonhyperdiploid ALL, consistent with prior direct measurements of FPGS activity [3, 17, 37]. The importance of GGH as a determinant of lineage differences in MTXPG was less clear. GGH activity estimates did not differ by lineage but were lower in hyperdiploid ALL blasts. We have ongoing studies to directly measure GGH in lysosomes of ALL blasts, because GGH activity is highest in lysosomes [47], and lysosomal transport of polyglutamates is likely to be important. High FPGS coupled with low GGH activity predicted higher MTXPG accumulation ex vivo and in vitro [15, 24, 25]. The model parameters were estimated using MTXPG concentrations measured in circulating ALL blasts, as it would have been impossible to perform multiple bone marrow aspirates over a 2-day period. Although this sampling overrepresents patients with high circulating blast counts, the model parameter estimates resulted in well-predicted MTXPGs in post-therapy bone marrow blast measures (e.g. Fig. 6).

One of the reasons to create a mathematical model is to test its predictions for alternative dosage schedules. The model indicated that increases in MTX dose beyond 2.5 g/m^2 would produce a minimal increase ($< 14\%$) in total MTXPG accumulation in ALL blasts. MTXPG accumulation has been observed to be saturable [14, 32], at about 10 μM extracellular MTX, in cultured H35 hepatoma cells. This concentration falls somewhat below the 30 μM plasma MTX that corresponds to a 2.5 g/m^2 dose, the approximate threshold dose predicted to be associated with saturation in our model (Fig. 7). The model also predicted that increasing the MTX dose could not completely overcome the MTXPG accumulation defect in T-cell ALL relative to B-lineage ALL, although increases in dose were predicted to result in further increases in MTXPG concentrations, but not proportional to the dose increase. Finally, the model indicated that in T-lineage ALL, longer infusion times led to higher (up to 28%) total MTXPG accumulation when the infusion time was increased from 4 h to 24 h. Whether these predictions will be borne out remains to be tested in additional clinical trials. These in vivo estimates of MTX disposition in blasts provide new insights toward determining the appropriate dose and infusion time of MTX in children with ALL, and indicate that the optimal dose and schedule may differ according to the lineage and ploidy subtype of ALL.

Acknowledgements We thank our clinical staff for scrupulous attention to patient care and management of bone marrow and blood sampling; our research nurses, Sheri Ring, Lisa Walters, Terri Kuehner, Margaret Edwards, and Paula Condy; and the patients and their parents for their participation in this study. We also thank Kathryn Brown, Nicole Roy, Michael Shipman, Eve Su, YaQin Chu, May Chung, Margaret Needham, Emily Melton, and Anatoliy Lenchik for technical assistance, and Nancy Kornegay for her computer and database expertise.

References

1. Allegra CJ, Chabner BA, Drake JC, Lutz R, Rodbard D, Jolivet J (1985) Enhanced inhibition of thymidylate synthase by methotrexate polyglutamates. J Biol Chem 260:9720
2. Allegra CJ, Drake JC, Jolivet J, Chabner BA (1985) Inhibition of phosphoribosylaminoimidazolecarboxamide transformylase by methotrexate and dihydrofolic acid polyglutamates. Proc Natl Acad Sci U S A 82:4881
3. Barredo JC, Synold TW, Laver J, Relling MV, Pui C-H, Priest DG, Evans WE (1994) Differences in constitutive and post-methotrexate folylpolyglutamate synthetase activity in B-lineage and T-lineage leukemia. Blood 84:564
4. Belkov VM, Krynetski EY, Schuetz JD, Yanishevski Y, Masson E, Mathew S, Raimondi S, Pui CH, Relling MV, Evans WE (1999) Reduced folate carrier expression in acute lymphoblastic leukemia: a mechanism for ploidy but not lineage differences in methotrexate accumulation. Blood 93:1643
5. Bertino JR (1993) Karnofsky memorial lecture. Ode to methotrexate. J Clin Oncol 11:5
6. Bertino JR, Goker E (1993) Drug resistance in acute leukemia. Leuk Lymphoma 11 [Suppl 2]:37
7. Camitta B, Leventhal B, Lauer S, Shuster JJ, Adair S, Casper J, Civin C, Graham M, Mahoney D, Munoz L, et al (1989) Intermediate-dose intravenous methotrexate and mercaptopurine therapy for non-T, non-B acute lymphocytic leukemia of childhood: a Pediatric Oncology Group study. J Clin Oncol 7:1539
8. Camitta B, Mahoney D, Leventhal B, Lauer SJ, Shuster JJ, Adair S, Civin C, Munoz L, Steuber P, Strother D, et al (1994) Intensive intravenous methotrexate and mercaptopurine treatment of higher-risk non-T, non-B acute lymphocytic leukemia: a Pediatric Oncology Group study. J Clin Oncol 12:1383
9. Chabner BA (1982) Methotrexate. In: Chabner BA (ed) Pharmacologic principles of cancer treatment. Saunders, Philadelphia, p 229
10. D'Argenio DZ, Schumitzky A (1997) ADAPT II user's guide: pharmacokinetic/pharmacodynamic systems analysis software. Biomedical Simulations Resource, Department of Biomedical Engineering, University of Southern California, Los Angeles
11. Evans WE, Relling MV, Rodman JH, Crom WR, Boyett JM, Pui CH (1998) Conventional compared with individualized chemotherapy for childhood acute lymphoblastic leukemia. N Engl J Med 338:499
12. Fry DW, Anderson LA, Borst M, Goldman ID (1983) Analysis of the role of membrane transport and polyglutamation of methotrexate in gut and the Ehrlich tumor in vivo as factors in drug sensitivity and selectivity. Cancer Res 43:1087
13. Galivan J, Balinska M (1983) Studies of formation and efflux of methotrexate polyglutamates with cultured hepatic cells. Adv Exp Med Biol 163:235
14. Galivan J, Nimec Z, Coward JK, McGuire JJ (1985) Glutamylation of methotrexate in hepatoma cells in vitro: regulation and the development of specific inhibitors. Adv Enzyme Regul 23:13
15. Galivan J, Johnson T, Rhee M, McGuire JJ, Priest D, Kesevan V (1987) The role of folylpolyglutamate synthetase and gamma-glutamyl hydrolase in altering cellular folyl- and antifolyl-polyglutamates. Adv Enzyme Regul 26:147

16. Galivan J, Ryan T, Rhee M, Yao R, Chave K (1999) Glutamyl hydrolase: properties and pharmacologic impact. Semin Oncol 26:33
17. Galpin AJ, Schuetz JD, Masson E, Yanishevski Y, Synold TW, Barredo JC, Pui CH, Relling MV, Evans WE (1997) Differences in folylpolyglutamate synthetase and dihydrofolate reductase expression in human B-lineage versus T-lineage leukemic lymphoblasts: mechanisms for lineage differences in methotrexate polyglutamylation and cytotoxicity. Mol Pharmacol 52:155
18. Gorlick R, Goker E, Trippett T, Waltham M, Banerjee D, Bertino JR (1996) Intrinsic and acquired resistance to methotrexate in acute leukemia. N Engl J Med 335:1041
19. Gorlick R, Goker E, Trippett T, Steinherz P, Elisseyeff Y, Mazumdar M, Flintoff WF, Bertino JR (1997) Defective transport is a common mechanism of acquired methotrexate resistance in acute lymphocytic leukemia and is associated with decreased reduced folate carrier expression. Blood 89:1013
20. Jackson RC, Harrap KR (1973) Studies with a mathematical model of folate metabolism. Arch Biochem Biophys 158:827
21. Kamen BA, Bertino JR (1980) Folate and anti-folate transport in mammalian cells. Antibiot Chemother 28:62
22. Kamen BA, Capdevila A (1986) Receptor-mediated folate accumulation is regulated by the cellular folate content. Proc Natl Acad Sci U S A 83:5983
23. Kennedy DG, van den Berg HW, Clarke R, Murphy RF (1985) The effect of leucovorin on the synthesis of methotrexate polygamma- glutamates in the MCF-7 human breast cancer cell line. Biochem Pharmacol 34:2897
24. Longo GS, Gorlick R, Tong WP, Ercikan E, Bertino JR (1997) Disparate affinities of antifolates for folylpolyglutamate synthetase from human leukemia cells. Blood 90:1241
25. Longo GS, Gorlick R, Tong WP, Lin S, Steinherz P, Bertino JR (1997) Gamma-Glutamyl hydrolase and folylpolyglutamate synthetase activities predict polyglutamylation of methotrexate in acute leukemias. Oncol Res 9:259
26. Mahoney DH Jr, Shuster J, Nitschke R, Lauer SJ, Winick N, Steuber CP, Camitta B (1998) Intermediate-dose intravenous methotrexate with intravenous mercaptopurine is superior to repetitive low-dose oral methotrexate with intravenous mercaptopurine for children with lower-risk B-lineage acute lymphoblastic leukemia: a Pediatric Oncology Group Phase III trial. J Clin Oncol 16:246
27. Masson E, Relling MV, Synold TW, Liu Q, Schuetz JD, Sandlund JT, Pui CH, Evans WE (1996) Accumulation of methotrexate polyglutamates in lymphoblasts is a determinant of antileukemic effects in vivo. A rationale for high-dose methotrexate. J Clin Invest 97:73
28. Matherly LH, Taub JW, Ravindranath Y, Proefke SA, Wong SC, Gimotty P, Buck S, Wright JE, Rosowsky A (1995) Elevated dihydrofolate reductase and impaired methotrexate transport as elements in methotrexate resistance in childhood acute lymphoblastic leukemia. Blood 85:500
29. Moran RG (1983) Characterization of the function of mammalian folylpolyglutamate synthetase (FPGS). Adv Exp Med Biol 163:327
30. Morrison PF, Allegra CJ (1987) The kinetics of methotrexate polyglutamation in human breast cancer cells. Arch Biochem Biophys 254:597
31. Niemeyer CM, Gelber RD, Tarbell NJ, Donnelly M, Clavell LA, Blattner SR, Donahue K, Cohen HJ, Sallan SE (1991) Low-dose versus high-dose methotrexate during remission induction in childhood acute lymphoblastic leukemia (protocol 81-01 update). Blood 78:2514
32. Nimec Z, Galivan J (1983) Regulatory aspects of the glutamylation of methotrexate in cultured hepatoma cells. Arch Biochem Biophys 226:671
33. Panetta JC, Wall A, Pui C-H, Evans WE (2002) Methotrexate intracellular disposition in acute lymphoblastic leukemia: a mathematical model of γ-glutamyl hydrolase activity. Clin Cancer Res 8:2423
34. Pui CH, Evans WE (1998) Acute lymphoblastic leukemia. N Engl J Med 339:605
35. Reiter A, Schrappe M, Wolf-Dieter L, Hiddemann W, Sauter S, Henze G, Zimmermann M, Lampert F, Havers W, Niethammer D, Odenwald E, Ritter J, Mann G, Welte K, Gadner H, Riehm H (1994) Chemotherapy in 998 unselected childhood acute lymphoblastic leukemia patients. Results and conclusions of the multicenter trial ALL-BFM 86. Blood 84:3122
36. Rhee MS, Lindau-Shepard B, Chave KJ, Galivan J, Ryan TJ (1998) Characterization of human cellular gamma-glutamyl hydrolase. Mol Pharmacol 53:1040
37. Rots MG, Pieters R, Peters GJ, Noordhuis P, van Zantwijk CH, Kaspers GJ, Hahlen K, Creutzig U, Veerman AJ, Jansen G (1999) Role of folylpolyglutamate synthetase and folylpolyglutamate hydrolase in methotrexate accumulation and polyglutamylation in childhood leukemia. Blood 93:1677
38. Rots MG, Pieters R, Peters GJ, Noordhuis P, van Zantwijk CH, Henze G, Janka-Schaub GE, Veerman AJ, Jansen G (2000) Methotrexate resistance in relapsed childhood acute lymphoblastic leukaemia. Br J Haematol 109:629
39. Samuels LL, Goutas LJ, Priest DG, Piper JR, Sirotnak FM (1986) Hydrolytic cleavage of methotrexate gamma-polyglutamates by folylpolyglutamyl hydrolase derived from various tumors and normal tissues of the mouse. Cancer Res 46:2230
40. Schorin MA, Blattner S, Gelber RD, Tarbell NJ, Donnelly M, Dalton V, Cohen HJ, Sallan SE (1994) Treatment of childhood acute lymphoblastic leukemia: results of Dana-Farber Cancer Institute/Children's Hospital Acute Lymphoblastic Leukemia Consortium Protocol 85-01. J Clin Oncol 12:740
41. Synold TW, Relling MV, Boyett JM, Rivera GK, Sandlund JT, Mahmoud H, Crist WM, Pui CH, Evans WE (1994) Blast cell methotrexate-polyglutamate accumulation in vivo differs by lineage, ploidy, and methotrexate dose in acute lymphoblastic leukemia. J Clin Invest 94:1996
42. White JC (1979) Reversal of methotrexate binding to dihydrofolate reductase by dihydrofolate. Studies with pure enzyme and computer modeling using network thermodynamics. J Biol Chem 254:10889
43. White JC, Goldman ID (1981) Methotrexate resistance in al L1210 cell line resulting from increased dihydrofolate reductase, decreased thymidylate synthetase activity, and normal membrane transport. Computer simulations based on network thermodynamics. J Biol Chem 256:5722
44. White JC, Mikulecky DC (1981) Application of network thermodynamics to the computer modeling of the pharmacology of anticancer agents: a network model for methotrexate action as a comprehensive example. Pharmacol Ther 15:251
45. Whitehead VM, Rosenblatt DS, Vuchich MJ, Shuster JJ, Witte A, Beaulieu D (1990) Accumulation of methotrexate and methotrexate polyglutamates in lymphoblasts at diagnosis of childhood acute lymphoblastic leukemia: a pilot prognostic factor analysis. Blood 76:44
46. Whitehead VM, Vuchich MJ, Lauer SJ, Mahoney D, Carroll AJ, Shuster JJ, Esseltine DW, Payment C, Look AT, Akabutu J, et al (1992) Accumulation of high levels of methotrexate polyglutamates in lymphoblasts from children with hyperdiploid (greater than 50 chromosomes) B-lineage acute lymphoblastic leukemia: a Pediatric Oncology Group study. Blood 80:1316
47. Yao R, Rhee MS, Galivan J (1995) Effects of gamma-glutamyl hydrolase on folyl and antifolylpolyglutamates in cultured H35 hepatoma cells. Mol Pharmacol 48:505
48. Yao R, Schneider E, Ryan TJ, Galivan J (1996) Human gamma-glutamyl hydrolase: cloning and characterization of the enzyme expressed in vitro. Proc Natl Acad of Sci U S A 93:10134